Discovery of exceptional points in the Bose-Einstein condensation of gases with attractive $1/r$ interaction

Holger Cartarius,* Jörg Main, and Günter Wunner
Institut für Theoretische Physik 1, Universität Stuttgart, D-70550 Stuttgart, Germany
(Received 21 September 2007; published 25 January 2008)

The extended Gross-Pitaevskii equation for the Bose-Einstein condensation of gases with attractive $1/r$ interaction has a second solution which is born together with the ground state in a tangent bifurcation. At the bifurcation point both states coalesce, i.e., the energies and the wave functions are identical. We investigate the bifurcation point in the context of exceptional points, a phenomenon known for linear non-Hermitian Hamiltonians. We point out that the mean field energy, the chemical potential, and the wave functions show the same behavior as an exceptional point in a linear, nonsymmetric system. The analysis of the analytically continued Gross-Pitaevskii equation reveals complex waves at negative scattering lengths below the tangent bifurcation. These solutions are interpreted as a decay of the condensate caused by an absorbing potential.

DOI: 10.1103/PhysRevA.77.013618 PACS number(s): 03.75.Hh, 02.30.−f, 34.20.Cf, 04.40.−b

I. INTRODUCTION

It is a well known property of Bose-Einstein condensates with attractive interatomic interactions that stationary solutions to the Gross-Pitaevskii equation exist only in certain regions of the parameter space governing the physics of the condensates. For example, for the case of an attractive *s*-wave contact interaction it was theoretically predicted (see, e.g., Refs. [1–3]), and experimentally confirmed [4–6], that the condensate collapses when, for given negative scattering length, the number of particles becomes too large. In an alternative experiment [7] the collapse was induced by tuning the scattering length in the vicinity of Feshbach resonances by adjusting an external magnetic field. Huepe *et al.* [8,9] have shown that the critical parameter values where collapse occurs in fact correspond to bifurcation points of the solutions to the stationary Gross-Pitaevskii equation and analyzed the linear stability of the solutions. Quite recently it was demonstrated [10] that similar behavior persists in Bose-Einstein condensates where, in addition to the short-range (van der Waals–like) interaction a long-range "gravitylike" attractive $1/r$ interaction is present. Such monopolar quantum gases could be realized according to O'Dell *et al.* [11] by a combination of six appropriately arranged "triads" of intense off-resonant laser beams. There, too, when crossing the borderlines in the parameter space, spanned by particle number, scattering length, and trap frequency, at which a stationary ground state of the extended Gross-Pitaevskii equation comes into being, a second, excited, state of the condensate is born in a tangent bifurcation.

It is the purpose of this paper to examine these bifurcations from the point of view of the theory of "exceptional points," since at the bifurcation points both the eigenvalues and the wave functions of the two states are identical, a situation well known from studies of exceptional points [12], which have been investigated theoretically [13–20] and experimentally [21–25] in a wide variety of physical systems.

Exceptional points can appear in systems described by non-Hermitian matrices which depend on a two-dimensional parameter space. At critical points in the parameter space (exceptional points) a coalescence of two eigenstates can occur, where *both* the eigenvalues *and* the eigenvectors of the two states pass through a branch point singularity and become identical. There is only one linearly independent eigenvector of the two states at the exceptional point.

In the quantum mechanics of linear Schrödinger equations, exceptional points are investigated in open systems in which resonances exist. Examples are discussed, e.g., for complex atoms in laser fields [26], a double δ well [27], the scattering of a beam of particles by a double barrier potential [28], and the hydrogen atom in static external fields [29]. The existence of resonances is important for the occurrence of exceptional points in quantum systems because the coalescence of two eigenstates is not possible in the case of Hermitian Hamiltonians describing bound states. In the latter case, there is always a set of orthogonal eigenstates which never become identical. The situation is different for resonances, which can, e.g., be described by *non*-Hermitian Hamiltonians. In this case, the eigenstates have not to be orthogonal and a coalescence can occur.

In this paper we will reveal the existence of exceptional points also in quantum systems described by *nonlinear* Schrödinger equations. As a model system we choose Bose-Einstein condensates with attractive $1/r$ interaction and concentrate on the case of self-trapping, i.e., condensation without external trap, which is a feature of such systems [10,11]. It is shown that the bifurcations of the two stationary solutions to the nonlinear Gross-Pitaevskii equation at critical physical parameter values exhibit the typical structure known from studies of exceptional points in linear systems. We should point out that the effect is not restricted to condensates with $1/r$-interaction. Our model system has the great advantage that simple approximate analytic solutions exist, which can be used for the investigation of the exceptional points. The branch point singularity structure can be seen directly from the analytic terms we obtain, which is only possible for self-trapped condensates *without* external harmonic trap.

The Gross-Pitaevskii equation for self-trapped Bose-Einstein condensates with monopolar $1/r$ interaction is intro-

*Holger.Cartarius@itp1.uni-stuttgart.de

duced in Sec. II. In Sec. III, we give an overview on exceptional points in linear systems and their properties, which can be used to identify them. The complex vicinity of the bifurcation point is investigated in Sec. IV to reveal the branch point singularity structure of the bifurcation and to identify it as a "nonlinear version" of an exceptional point. The physical interpretation of a complex absorbing potential in the Gross-Pitaevskii equation at scattering lengths below the critical value at the tangent bifurcation is discussed in Sec. V. Conclusions are drawn in Sec. VI.

II. BOSE-EINSTEIN CONDENSATES WITH $1/r$ INTERACTION

In this section we briefly review the equations and results for self-trapped Bose-Einstein condensates with attractive $1/r$ interaction which are necessary for the subsequent analysis of exceptional points. The extended Gross-Pitaevskii equation without external trap potential reads

$$\left[-\Delta_{\boldsymbol{r}}+N\left(8\pi\frac{a}{a_u}|\psi(\boldsymbol{r})|^2-2\int d^3\boldsymbol{r}'\frac{|\psi(\boldsymbol{r}')|^2}{|\boldsymbol{r}-\boldsymbol{r}'|}\right)\right]\psi(\boldsymbol{r})=\varepsilon\psi(\boldsymbol{r}), \tag{1}$$

where the natural "atomic" units introduced in Ref. [10] were used. Lengths are measured in units of a "Bohr radius" a_u and energies in units of a "Rydberg energy" E_u, which are given by

$$a_u=\frac{\hbar^2}{mu},\quad E_u=\frac{\hbar^2}{2ma_u^2},$$

respectively, where u determines the strength of the atom-atom-interaction [11], and m is the mass of one boson. In Eq. (1), ε is the chemical potential, a is the s-wave scattering length, and N is the number of bosons. As was pointed out in Ref. [10] with the use of the scaling property of the system, the physics of a self-trapped condensate is only determined by one parameter, namely N^2a/a_u, which will be necessary for the identification of the exceptional point. A further quantity necessary for our discussions is the mean field energy of the self-trapped condensate, which reads

$$E[\psi]=N\int d^3\boldsymbol{r}\psi^*(\boldsymbol{r})\left(-\Delta_{\boldsymbol{r}}+4\pi N\frac{a}{a_u}|\psi(\boldsymbol{r})|^2-N\int d^3\boldsymbol{r}'\frac{|\psi(\boldsymbol{r}')|^2}{|\boldsymbol{r}-\boldsymbol{r}'|}\right)\psi(\boldsymbol{r}). \tag{2}$$

The solutions we are interested in, viz. the two states emerging at the tangent bifurcation, are radially symmetric. One of them is the ground state. Thus we concentrate on radially symmetric solutions of Eq. (1). In this case both analytic calculations via a variational method and numerically exact computations can be carried out.

A. Variational solutions

An analytic approximation for the two wave functions of the condensate which emerge at the tangent bifurcation can be obtained using a variational principle. Calculations with a Gaussian type orbital were performed by O'Dell *et al.* [11] and compared with numerically accurate solutions in Ref. [10]. The trial wave function is given by

$$\psi(\boldsymbol{r})=A\exp\left(-\frac{1}{2}k^2\boldsymbol{r}^2\right), \tag{3}$$

where

$$A=\left(\frac{k}{\sqrt{\pi}}\right)^{3/2} \tag{4}$$

is the normalization constant and the variation is performed with respect to the width represented by k. The two stationary values,

$$\frac{E_\pm}{N^3}=-\frac{4}{9\pi}\frac{1\pm2\sqrt{1+(8/3\pi)N^2(a/a_u)}}{[1\pm\sqrt{1+(8/3\pi)N^2(a/a_u)}]^2}, \tag{5}$$

of the mean field energy (2) are obtained at

$$k_\pm=\frac{1}{2}\sqrt{\frac{\pi}{2}}\frac{1}{N^2(a/a_u)}\left(\pm\sqrt{1+\frac{8}{3\pi}N^2\frac{a}{a_u}}-1\right). \tag{6}$$

E_+ represents the variational approximation for the ground state of the condensate, the second solution (excited state) is labeled E_-. Furthermore, the analytical expressions for the chemical potentials of the two solutions are given by

$$\frac{\varepsilon_\pm}{N^2}=-\frac{4}{9\pi}\frac{5\pm4\sqrt{1+(8/3\pi)N^2(a/a_u)}}{[1\pm\sqrt{1+(8/3\pi)N^2(a/a_u)}]^2}, \tag{7}$$

respectively. The tangent bifurcation is obvious from Eqs. (5) and (7). For negative scattering lengths with $N^2a/a_u<-3\pi/8$ there is no (real) result for E and ε, at the critical value $N^2a/a_u=-3\pi/8$ both solutions have the same value ($E_+=E_-$, $\varepsilon_+=\varepsilon_-$), and above $-3\pi/8$, we obtain two different real solutions. The variational chemical potential is shown as a function of the scattering length parameter N^2a/a_u in Fig. 1.

B. Exact calculations

For the search of radially symmetric wave functions, the radial part of the integrodifferential Eq. (1) is written in the form of two differential equations,

$$\Psi''(r)+\frac{2}{r}\Psi'(r)=-U(r)\Psi(r)+8\pi b|\Psi(r)|^2\Psi(r), \tag{8}$$

$$U''(r)+\frac{2}{r}U'(r)=-8\pi|\Psi(r)|^2, \tag{9}$$

with the parameter

$$b=\frac{a}{a_u}. \tag{10}$$

The N dependence in Eq. (1) has been absorbed in the wave function $\Psi=\sqrt{N}\psi$. The two second order differential equations can be transformed to first order equations and integrated, e.g., with a Runge-Kutta-Merson algorithm starting

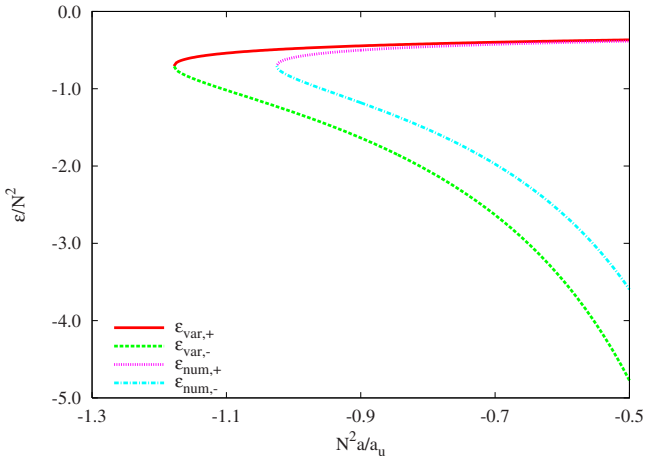

FIG. 1. (Color online) Chemical potentials of the two solutions. The results of the variational and the numerical exact calculations are shown. Two solutions emerge in a tangent bifurcation at a critical value of the parameter N^2a/a_u. In the variational approximation the critical value is $N^2a/a_u=-3\pi/8$, whereas the numerical exact solutions emerge at $N^2a/a_u=-1.0251$ [10]. The "atomic" units introduced in Ref. [10] are used.

at, e.g., $\tilde{r}_0=10^{-19}$ slightly greater than zero with the initial conditions

$$\tilde{\Psi}(\tilde{r}_0)=1, \quad \tilde{\Psi}'(\tilde{r}_0)=0, \quad \tilde{U}(\tilde{r}_0)=u_0, \quad \tilde{U}'(\tilde{r}_0)=0. \tag{11}$$

The value u_0 must be determined such that $\tilde{\Psi}(\tilde{r})$ vanishes in the limit $\tilde{r}\to\infty$. Numerically, integration up to $\tilde{r}_{\max}\approx 15$ is sufficient. The wave function obtained with the initial condition $\tilde{\Psi}(\tilde{r}_0)=1$ is not normalized, which is indicated with the tilde. Because of the scaling property [10] of the problem, the normalization of a numerically obtained solution $\tilde{\Psi}$ is possible with the help of a normalization factor ν. As can be seen with a simple calculation, the transformation

$$(\Psi,r,\varepsilon,a)\to\left(\nu^2\Psi,\frac{r}{\nu},\nu^2\varepsilon,\frac{a}{\nu^2}\right) \tag{12}$$

leaves the system (8) and (9) of differential equations invariant. With the normalization condition $\|\Psi\|^2=N$ and the scaling invariance (12), the normalization factor is given by

$$\left(\frac{\nu}{N}\right)^{-1}=\|\tilde{\Psi}\|^2=4\pi\int_0^\infty|\tilde{\Psi}(\tilde{r})|^2\tilde{r}^2d\tilde{r} \tag{13}$$

and the properly scaled and normalized wave function $\Psi(r)$ is obtained as

$$\Psi(r)=\nu^2\tilde{\Psi}(\tilde{r}/\nu) \tag{14}$$

with the scaled scattering length

$$N^2\frac{a}{a_u}=\frac{b}{\nu^2}. \tag{15}$$

An explicit calculation of the integral (13) is not required. Using the asymptotic behavior of the numerically computed potential $\tilde{U}(\tilde{r})$ for large radial coordinates

$$\tilde{U}(\tilde{r})\approx\tilde{\varepsilon}+2\frac{N}{\nu}\frac{1}{\tilde{r}}, \tag{16}$$

the factor ν/N can be calculated from

$$\frac{\nu}{N}=\lim_{\tilde{r}\to\infty}\frac{-2}{\tilde{r}^2\tilde{U}'(\tilde{r})}. \tag{17}$$

The correctly scaled chemical potential can also be determined with the help of the approximation (16):

$$\frac{\varepsilon}{N^2}=\left(\frac{\nu}{N}\right)^2\lim_{\tilde{r}\to\infty}[\tilde{U}(\tilde{r})+\tilde{r}\tilde{U}'(\tilde{r})]. \tag{18}$$

Only for the mean field energy a further integral is required. Using the virial theorem [1,11] we can obtain it as

$$\frac{E}{N^3}=-\frac{\langle U\rangle}{N^2}=-4\pi\left(\frac{\nu}{N}\right)^3\int_0^\infty|\tilde{\Psi}(\tilde{r})|^2\tilde{U}(\tilde{r})\tilde{r}^2d\tilde{r}. \tag{19}$$

The numerical exact chemical potential is also shown in Fig. 1. It agrees, qualitatively, with the result of the variational approach, however, the tangent bifurcation is shifted to a higher critical scattering length $N^2a/a_u=-1.0251$ [10].

We will show in Sec. IV that in both the variational approach and the exact calculations the tangent bifurcation at the critical scattering length is a branch point singularity of the wave functions, i.e., an *exceptional point*.

III. EXCEPTIONAL POINTS

To make our presentation self-contained we recapitulate the essential concepts on exceptional points and their properties known from linear systems, which will be important for the comparison with the coalescence of two quantum states in a nonlinear Schrödinger equation in Sec. IV. Usually complex symmetric matrices or complex symmetric matrix representations of Hamiltonians are used to investigate exceptional points in quantum systems (see, e.g., Refs. [15,27,29]). Here, we treat the more general case of nonsymmetric matrices, considered before [30–32] also for systems with time reversal symmetry breaking [33–35], and compare the phase behavior of the eigenvectors with the symmetric case. It is instructive to discuss a simple two-dimensional model which exhibits exceptional points. The example is provided by the 2×2 matrix

$$\boldsymbol{M}(\lambda)=\begin{pmatrix}1 & \lambda\\ c+\lambda & -1\end{pmatrix}. \tag{20}$$

In Eq. (20), λ is a complex parameter, and the complex number c is introduced to distinguish between the general nonsymmetric case ($c\neq 0$) and a symmetric matrix ($c=0$) in the discussion below. The eigenvalues read

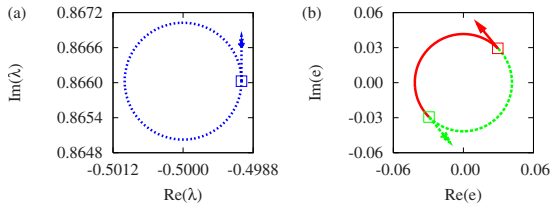

FIG. 2. (Color online) Eigenvalues of the two-dimensional model defined in Eq. (20) with $c=1$ for a circle around the exceptional point. (a) Circle in the parameter space with radius $\varrho=10^{-3}$. The starting point $\lambda(0)$ is marked with an open square and the direction of progression is indicated with the arrow. (b) Path of the eigenvalues $e_{1,2}$ for the parameter values on the circle. The eigenvalues which belong to the first parameter value $\lambda(0)$ are labeled with open squares and the arrows point in the direction of progression.

$$e_{1,2}(\lambda) = \pm\sqrt{1+c\lambda+\lambda^2} \tag{21}$$

and are obviously two branches of one analytic function. Corresponding non-normalized eigenvectors of the two eigenvalues are given by

$$\boldsymbol{x}_{1,2}(\lambda) = \begin{pmatrix} -\lambda \\ 1 \mp \sqrt{1+c\lambda+\lambda^2} \end{pmatrix}. \tag{22}$$

There are two exceptional points for $\lambda_{A,B}=-c/2\pm\sqrt{c^2/4-1}$. At these parameter values, both the eigenvalues $e_{1,2}$ and the eigenvectors $\boldsymbol{x}_{1,2}$ pass through a branch point singularity. For the further discussions we concentrate on the case $\lambda=\lambda_A$. Then the degenerate eigenvalues have the value $e_{1,2}(\lambda_A)=0$ and the two eigenvectors $\boldsymbol{x}_{1,2}$ are

$$\boldsymbol{x}_{1,2}(\lambda_A) = \begin{pmatrix} c/2-\sqrt{c^2/4-1} \\ 1 \end{pmatrix}. \tag{23}$$

An important property of exceptional points, which follows from the branch point singularity structure, is the permutation of the two eigenvalues if the exceptional point is encircled in the parameter space [12]. To illustrate this effect we follow the paths of the eigenvalues $e_{1,2}$ in the complex plane for a circle with radius ϱ around the critical value λ_A, which can be represented by

$$\lambda_\varrho(\varphi) = -c/2+\sqrt{c^2/4-1}+\varrho e^{i\varphi}. \tag{24}$$

An approximation for small radii $\varrho \ll |2\sqrt{c^2/4-1}|$ leads to

$$e_1(\lambda_\varrho(\varphi)) = \sqrt{2\varrho\sqrt{c^2/4-1}}e^{i(\varphi/2+\pi/4)},$$

$$e_2(\lambda_\varrho(\varphi)) = \sqrt{2\varrho\sqrt{c^2/4-1}}e^{i(\varphi/2+5\pi/4)}. \tag{25}$$

If a full circle in the complex parameter space λ is traversed, the paths of the eigenvalues form a semicircle as can be seen from Eq. (25). Neither of the two eigenvalues passes through a closed loop. The first arrives, after the parameter space loop, at the starting point of the second one and vice versa. Two circles in the λ space ($\varphi=0\cdots4\pi$) are required to obtain a full circle of *one* of the eigenvalues. The situation is shown in Fig. 2 for $c=1$. In the parameter space the circle (24) is traversed once with a radius $\varrho=10^{-3}$, as plotted in Fig. 2(a). The paths of the two eigenvalues in the complex e space is shown in Fig. 2(b). The semicircle structure expected from approximation (25) is clearly visible.

For exceptional points in linear systems there is a noteworthy difference for complex symmetric and nonsymmetric matrices. In the first case, which is obtained for $c=0$ in the model (20) and which was realized in the resonances investigated in microwave cavities [22] and in the hydrogen atom in crossed electric and magnetic fields [29], there is always a distinct phase behavior of the eigenvectors. If an exceptional point is encircled, the two eigenvectors are interchanged (as expected from the behavior of the energy eigenvalues) and, additionally, *one* of the two eigenvectors changes its sign. This effect is demonstrated in Ref. [15] and can be summarized with, e.g.,

$$[\boldsymbol{x}_1,\boldsymbol{x}_2] \overset{\text{circle}}{\rightarrow} [-\boldsymbol{x}_2,\boldsymbol{x}_1]. \tag{26}$$

Four circles around the exceptional point in the parameter space are needed to restore the original situation $[\boldsymbol{x}_1,\boldsymbol{x}_2]$. A direct verification of the effect was performed with microwave cavity experiments [22], in which a visualization of the wave functions was possible. The phase behavior can be obtained for the vectors $\boldsymbol{x}_i$ normalized with the Euclidean norm without complex conjugation $N_i=\sqrt{\boldsymbol{x}_i^T\boldsymbol{x}_i}$, where $\boldsymbol{x}_i^T$ is the transpose of the vector $\boldsymbol{x}_i$ (cf. Ref. [20]). This normalization fixes the phase and is the method required for the comparison with the nonlinear system studied in this paper (cf. Sec. IV and the Appendix).

For the nonsymmetric case the change in sign does not appear for a vector whose phase has been fixed with the same method, i.e., the Euclidean norm without complex conjugation. A nonsymmetric matrix is obtained in the model (20) for $c\neq0$. Then, there is only a permutation of the eigenvectors, which can be summarized with

$$[\boldsymbol{x}_1,\boldsymbol{x}_2] \overset{\text{circle}}{\rightarrow} [\boldsymbol{x}_2,\boldsymbol{x}_1]. \tag{27}$$

This is shown analytically for a small circle in the Appendix. Note that the phase behavior (27) does not represent the "geometric phase" of an eigenvector during the circle around an exceptional point, which has been calculated in Ref. [31].

A demonstration of the phase behavior is possible with the product

$$p_{12} = \boldsymbol{x}_1^T\begin{pmatrix} 0 & 1 \\ 1 & 0 \end{pmatrix}\boldsymbol{x}_2. \tag{28}$$

The nondiagonal matrix ensures that the product p_{12} does not vanish in the symmetric case. If the change in sign is present, the phase of p_{12} changes its value by π when a full circle around the exceptional point is traversed. In Fig. 3 the behavior of the product is shown for the example (20). The change in sign is obvious in the symmetric case $c=0$ and does not appear for the nonsymmetric choice $c=1$.

IV. ANALYTIC CONTINUATION OF THE GROSS-PITAEVSKII SYSTEM

In the extended Gross-Pitaevskii Eq. (1), both the variational and the numerical calculations suggest the existence of

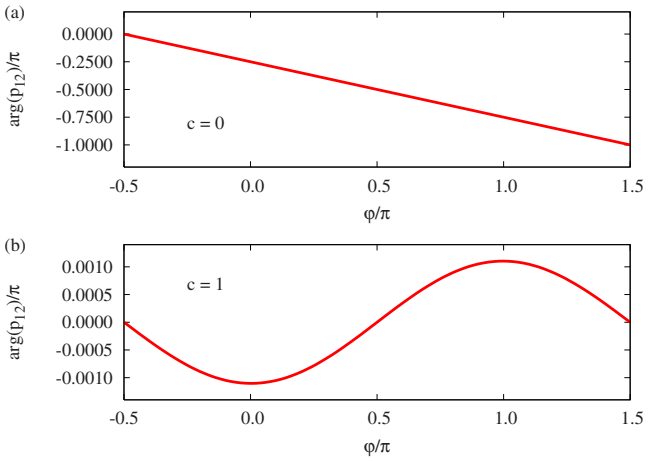

FIG. 3. (Color online) Phase of the product p_{12} for a circle in the parameter space of type (24) with radius $\varrho=10^{-3}$ around the exceptional point. (a) Symmetric matrix with $c=0$. The phase changes by π indicating the change in sign of one of the eigenvectors from Eq. (26). (b) Nonsymmetric matrix with $c=1$. There is no change in sign as noted in Eq. (27).

an exceptional point at the tangent bifurcation. For the critical parameter value, we obtain two identical states. The chemical potentials, the mean field energies, and the wave functions are identical. In contrast to exceptional points in linear systems described in Sec. III the coalescence of the two states of the nonlinear Schrödinger Eq. (1) can appear for a purely real wave function at a real energy in a one-dimensional parameter space. This is a consequence of the nonlinearity of the Schrödinger equation.

If we want to check whether or not the degeneracy in the nonlinear system has the same branch point singularity structure as exceptional points in open quantum systems described by a linear Schrödinger equation, we have to extend the parameter N^2a/a_u to complex values and to investigate the complex vicinity of the degeneracy.

The analytic continuation of the Gross-Pitaevskii system is a nontrivial task. The Gross-Pitaevskii Eq. (1) contains the square modulus of the wave function ψ and is therefore a nonanalytic function of ψ. It has been argued that the tempting simple replacement of $|\psi|^2$ with ψ^2 is valid only with the assumption that the entire wave function is real valued [36,37]. Here, we suggest the following procedure for complex wave functions.

Any complex wave function can be written as

$$\psi(\boldsymbol{r}) = e^{\alpha(\boldsymbol{r})+i\beta(\boldsymbol{r})}, \tag{29}$$

where the real functions $\alpha(\boldsymbol{r})$ and $\beta(\boldsymbol{r})$ determine the amplitude and phase of the wave function, respectively. The complex conjugate and the square modulus of $\psi(\boldsymbol{r})$ read

$$\psi^*(\boldsymbol{r}) = e^{\alpha(\boldsymbol{r})-i\beta(\boldsymbol{r})}, \quad |\psi(\boldsymbol{r})|^2 = e^{2\alpha(\boldsymbol{r})}. \tag{30}$$

Using the ansatz (29) the Gross-Pitaevskii system can be written as two coupled nonlinear differential equations for $\alpha(\boldsymbol{r})$ and $\beta(\boldsymbol{r})$, however, without any complex conjugate or square modulus. These equations can now be continued analytically by allowing for complex valued functions $\alpha(\boldsymbol{r})$ and $\beta(\boldsymbol{r})$. This implies that Eq. (30) *without* complex conjugate of $\alpha(\boldsymbol{r})$ and $\beta(\boldsymbol{r})$ is formally used for the calculation of ψ^* and $|\psi(\boldsymbol{r})|^2$, and thus the square modulus of ψ can become complex. The physical interpretation of a complex absorbing potential in the Gross-Pitaevskii system will be discussed below in Sec. V.

It should be noted that the above procedure is analogous to the complex scaling method, viz. the replacement $r \to re^{i\theta}$ in the Hamiltonian, used for the calculation of resonances in open quantum systems [38,39]. For states on the left hand side of operators there is no complex conjugation of the $re^{i\theta}$ arising from the scale transformation but complex conjugation is applied to the intrinsically complex part of the function.

In the following we will encircle the branch point singularity at the tangent bifurcation. For the variational approach discussed in Sec. II A, Eqs. (5)–(7) are straightforwardly extended to complex values of the parameter N^2a/a_u, yielding complex results for the chemical potential, the mean field energy, and the wave functions. The situation is more complicated for the exact calculations in Sec. II B because the differential Eqs. (8) and (9) do not directly depend on the scaled scattering length N^2a/a_u but on the parameter b. For complex b the differential Eqs. (8) and (9) can be continued analytically resulting in complex wave functions. Then, the two complex parameters u_0 and b are determined in a multidimensional root search problem, to fulfill the condition of vanishing wave function in the limit $r\to\infty$, and to achieve the given value of N^2a/a_u.

A. Branch point singularity structure of the energies

The variational solutions (5) for the mean field energy and Eq. (7) for the chemical potential show a branch point singularity at the bifurcation point. For a circle around the critical value of the complex parameter N^2a/a_u the typical permutation of the two solutions is expected and found, as is shown in Fig. 4 for the variational approximation as well as for the numerical exact calculations. The circle in the parameter space is defined by

$$N^2a/a_u = (N^2a/a_u)_c + \varrho e^{i\varphi}, \quad \varphi = 0 \cdots 2\pi, \tag{31}$$

where $(N^2a/a_u)_c$ is set to the critical value $(N^2a/a_u)_{var} = -3\pi/8 = -1.1780$ in the variational and to $(N^2a/a_u)_{num} = -1.0251$ in the numerical exact calculations, respectively. We used the radius $\varrho=10^{-3}$. Both cases are shown in Figs. 4(a) and 4(b). In Figs. 4(c) and 4(d) the variational and numerical solutions for the chemical potential are shown. The results were obtained for different parameter values located on the circle. As can be seen in the figure, the permutation of the two values of the chemical potential appears very clearly. Each of the two solutions ε_+ and ε_- traverses a path in the complex energy plane similar to a semicircle. A fractional power series expansion of the variational result (7) for small radii,

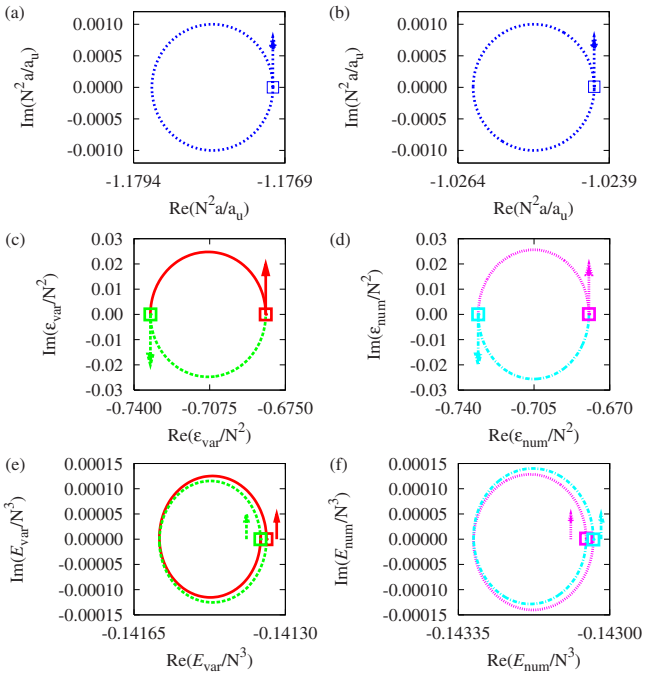

FIG. 4. (Color online) Chemical potential and mean field energy for a circle in the complex N^2a/a_u parameter space. The first row shows the parameter space circle of type (31) with $\varrho=10^{-3}$ used for the variational (a) and the numerical exact (b) calculations. The starting point is marked with an open square and the direction of progression is indicated with an arrow. In the second row, the chemical potential ε/N^2 for the variational (c) and numerical (d) solutions is plotted. The variational (e) and numerical (f) mean field energies E/N^3 are presented in the third row. Each of the two solutions is drawn with a different line. The results obtained for the first parameter value on the circle are marked with an open square and the arrows point in the direction of progression. A permutation of the two solutions is present for the mean field energy as well as for the chemical potential indicating the existence of an exceptional point. All energies are given in units of the "Rydberg energy" E_u mentioned in Sec. II.

$$\frac{\varepsilon_\pm}{N^2} = -\frac{20}{9\pi} \pm \frac{8}{3\pi}\sqrt{\varrho}e^{i\varphi/2} - \left(\frac{4}{3\pi} + \frac{128}{27\pi^2}\right)\sqrt{\varrho}^2 e^{i\varphi} \pm \left(\frac{8}{9\pi} - \frac{64}{9\pi^2}\right)\sqrt{\varrho}^3 e^{(3/2)i\varphi} + O(\sqrt{\varrho}^4), \tag{32}$$

confirms this finding. The term $\frac{8}{3\pi}\sqrt{\varrho}e^{i\varphi/2}$, which dominates the path of the eigenvalue for a value $\varrho \ll 1$, leads to a semicircle.

For the mean field energy the permutation is also present but the structure of the paths of the two solutions is different. As can be seen from the fractional power series expansion of the analytic solution (5),

$$\frac{E_\pm}{N^3} = -\frac{4}{9\pi} + 0\sqrt{\varrho}e^{i\varphi/2} + \frac{32}{27\pi^2}\sqrt{\varrho}^2 e^{i\varphi} \pm \left(\frac{4}{9\pi} - \frac{32}{9\pi^2}\right)\sqrt{\varrho}^3 e^{(3/2)i\varphi} + O(\sqrt{\varrho}^4), \tag{33}$$

the first order term with the phase term $e^{i\varphi/2}$ vanishes. The lowest non-vanishing order has the phase factor $e^{i\varphi}$, which leads to a closed curve for a complete circle in the parameter space ($\varphi=0\cdots 2\pi$). The third order term is the lowest order responsible for a permutation. As a consequence, it becomes more and more difficult to see a permutation for decreasing radii ϱ. Nevertheless, the permutation of the two values is present. The same result can be seen in Figs. 4(e) and 4(f). The dominating structure is given by the circle following from the second order term but the permutation is clearly visible even for the small radius $\varrho=10^{-3}$.

The exceptional point discussed here was discovered for a real value of the parameter N^2a/a_u, however, it is still an isolated point in the two-dimensional parameter space spanned by the real and imaginary parts of N^2a/a_u. This finding is in full agreement with non-Hermitian linear systems, in which the co-dimension of exceptional points is 2 (see, e.g., Ref. [30]). The analytic continuation is required to confirm the branch point singularity structure. As mentioned above, the appearance on the real axis is possible because of the nonlinearity of the Schrödinger equation.

B. Behavior of the wave functions

The eigenfunctions of the extended stationary Gross-Pitaevskii Eq. (1) are not orthogonal. They behave more like the eigenstates of a nonsymmetric linear system and the phase behavior (27) without a change in sign is expected. A possibility to check this is to calculate the complex overlap integral for the two nonorthogonal normalized states,

$$O_{12} = 4\pi \int_0^\infty \psi_1(r)\psi_2(r)r^2 dr, \tag{34}$$

for parameter values located on a circle of the type (24). For this calculation it is important to note that the numerical wave functions calculated with the method described above have a phase, which is fixed by the normalization factor ν determined by Eq. (13) without complex conjugation for the analytic continuation of the extended Gross-Pitaevskii model [cf. Eq. (30)]. A similar procedure is used for the variational result, where the normalization constant A in Eq. (4) is calculated with a normalization integral without complex conjugation.

If one of the two states changes its sign during the traversal of the loop, the phase of the complex value O_{12} changes its value by π similarly to the phase behavior of the product p_{12} from Eq. (28). If this is not the case, the phase returns to its original value at the end of the loop.

In Fig. 5 the phase of the integral (34) is plotted for the circle defined in Eq. (31) with radius $\varrho=10^{-3}$. The result shows clearly that the phase of O_{12} returns to its initial value after one circle around the exceptional point, demonstrating that no change in sign of the eigenvectors occurs. Thus the wave functions behave in the same way as for exceptional points in linear systems described by a nonsymmetric matrix (see Sec. III).

V. DECAY OF THE CONDENSATE

The Gross-Pitaevskii Eq. (1) depends on the scattering length N^2a/a_u of the contact potential. In Sec. IV that param-

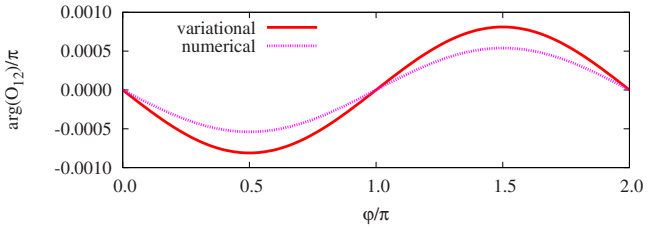

FIG. 5. (Color online) Phase $\arg(O_{12})$ of the overlap integral O_{12} defined in Eq. (34). The path in the parameter space N^2a/a_u is a circle with the critical value as center point and $\varrho=10^{-3}$. The angle on the circle is denoted by φ. Both the variational and the numerical results show that the phase of O_{12} returns to its initial value at the end of the circle and that the change in sign from Eq. (26) is not present as expected (see text).

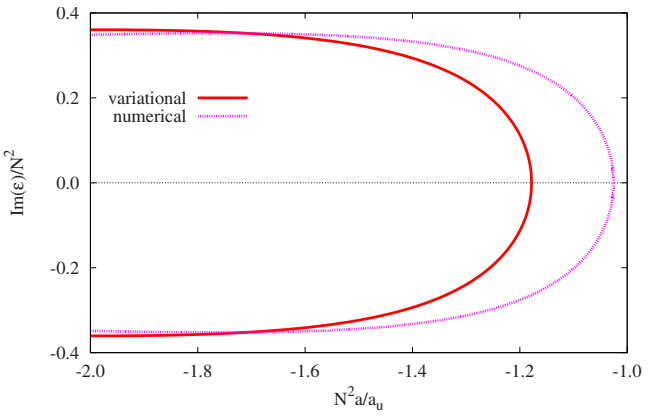

FIG. 6. (Color online) Imaginary part of the chemical potential for real N^2a/a_u below the bifurcation point obtained with the variational and the numerical calculations. Both the continuation of the ground state and the continuation of the excited state are plotted. One is the complex conjugate of the other.

eter has been extended to complex values, although the physical scattering length is always real. There is, however, a physical situation where complex continuation is needed for real N^2a/a_u, viz. when the scattering length is below the critical value at the tangent bifurcation. For $N^2a/a_u < -3\pi/8 = -1.1780$ the variational solutions (5) and (7) for the mean field energy and the chemical potential become complex. Those parameters become complex also for the analytically continued exact calculations at $N^2a/a_u < -1.0251$. A complex chemical potential as a signature of a decaying condensate has already been discussed in Ref. [40].

The standard physical interpretation of complex eigenenergies is that they describe decaying resonances in open systems or systems with absorbing potentials. The imaginary part of the energy E is related to the width Γ, decay rate λ, and lifetime T of the resonance by $\Gamma=\hbar\lambda=\hbar/T=-2\ \mathrm{Im}\ E$. Both the real and complex wave function of the Bose-Einstein condensate above and below the tangent bifurcation vanishes at large radius r, i.e., the wave function cannot describe a decay of the condensate by outgoing particles. How is a decay possible? The solution is that for a complex wave function $\psi(\boldsymbol{r})$, using the rules (30) for complex conjugate and square modulus, the effective potential

$$V_{\mathrm{eff}}(\boldsymbol{r}) = 8\pi N\frac{a}{a_u}|\psi(\boldsymbol{r})|^2 - 2N\int d^3\boldsymbol{r}'\frac{|\psi(\boldsymbol{r}')|^2}{|\boldsymbol{r}-\boldsymbol{r}'|} \qquad (35)$$

becomes an *absorbing* potential. Thus the decay is an internal collapse of the condensate. The physical interpretation might be that at large negative scattering lengths the contact potential is so attractive that the atoms of the condensate form molecules or clusters as discussed, e.g., in Refs. [7,40,41]. The decreasing number of atoms means the decay of the condensate. The imaginary part of the chemical potential as a function of the scattering length is presented in Fig. 6 for the variational as well as for the exact calculation. As was the case for parameter values above the critical point, there are two solutions. Below the critical N^2a/a_u one is the complex conjugate of the other.

VI. CONCLUSION

We have investigated the complex vicinity of the tangent bifurcation appearing in the extended Gross-Pitaevskii equation for self-trapped Bose-Einstein condensates with attractive $1/r$ interaction. The chemical potential and the mean field energy show the typical behavior of energies at an exceptional point. Both quantities pass through a branch point singularity at the critical value of the system's parameter N^2a/a_u. An analysis of the phase behavior of the corresponding wave functions showed that the bifurcation point has the same properties as an exceptional point of a non-Hermitian nonsymmetric matrix. Thus we conclude that we have identified the bifurcation point as a "nonlinear version" of an exceptional point.

For the investigation of the bifurcation point an analytic continuation of the Gross-Pitaevskii system was used. As we have discussed, an analytic continuation of the wave functions is not only required for complex values of N^2a/a_u but is necessary for real parameter values below the bifurcation point. Then, a complex absorbing effective potential is obtained indicating an internal collapse of the potential. An investigation of the dynamics of the system similar to Refs. [8,9] will give more insight in the stability of the states and is the topic of current studies.

In this paper we have identified the bifurcation points appearing in self-trapped monopolar Bose-Einstein condensates as exceptional points. There is good reason to believe that quite generally the critical parameter values of attractive Bose-Einstein condensates where collapse of the condensates sets in are associated with exceptional points. The existence of a bifurcation point is known for condensates in a harmonic trap without $1/r$ interaction [3,8] and for condensates with dipole-dipole interaction and harmonic trap. We have checked that the bifurcation points appearing in variational approximations of these systems are exceptional points. Clearly this should be confirmed by detailed analysis including numerically exact calculations for attractive Bose-Einstein condensates based on the techniques applied in this paper.

ACKNOWLEDGMENTS

This work was supported by Deutsche Forschungsgemeinschaft. H.C. is grateful for support from the Landesgraduiertenförderung of the Land Baden-Württemberg.

APPENDIX: PHASE OF THE EIGENVECTORS ON THE CIRCLE

To be able to compare the phase behavior of the wave functions of the nonlinear Gross-Pitaevskii system with the eigenvectors of a matrix, we fix the phase of the vectors with the same method as is discussed in Sec. IV for the wave functions of the analytic continuation of the extended Gross-Pitaevskii model. This is done with the Euclidean norm without complex conjugation $N_i=\sqrt{\boldsymbol{x}_i^T\boldsymbol{x}_i}$ of the eigenvectors, which is the adequate counterpart of the normalization factors ν from Eq. (13) and A from Eq. (4), where (formally) the complex conjugation is ignored. Then, the normalized eigenvectors have the form

$$\boldsymbol{x}_{1,2}(\lambda)=\frac{1}{N_{1,2}}\begin{pmatrix}-\lambda\\ 1\mp\sqrt{1+c\lambda+\lambda^2}\end{pmatrix}$$

with

$$N_{1,2}=\sqrt{\lambda^2+(1\mp\sqrt{1+c\lambda+\lambda^2})^2}.$$

For a small circle around the exceptional point $\lambda_A=-c/2+\sqrt{c^2/4-1}$ we calculate the fractional power series expansion in $\varrho^{1/4}$ of the normalized vectors and obtain in the nonsymmetric case ($c\neq 0$)

$$\boldsymbol{x}_1(\varphi)=\begin{pmatrix}\frac{1}{c}\sqrt{\eta/2}+\frac{2}{c}\sqrt{\kappa/\eta}\sqrt{\varrho}e^{i\varphi/2}+O(\varrho^{3/4})\\ \sqrt{2/\eta}-\frac{1}{c^2}\sqrt{\kappa\eta}\sqrt{\varrho}e^{i\varphi/2}+O(\varrho^{3/4})\end{pmatrix},$$

$$\boldsymbol{x}_2(\varphi)=\begin{pmatrix}\frac{1}{c}\sqrt{\eta/2}-\frac{2}{c}\sqrt{\kappa/\eta}\sqrt{\varrho}e^{i\varphi/2}+O(\varrho^{3/4})\\ \sqrt{2/\eta}+\frac{1}{c^2}\sqrt{\kappa\eta}\sqrt{\varrho}e^{i\varphi/2}+O(\varrho^{3/4})\end{pmatrix}$$

with $\kappa=\sqrt{c^2/4-1}$, and $\eta=c^2-2c\kappa$. The traversal of a single circle ($\varphi=0\cdots 2\pi$) obviously leads to a permutation of the eigenvectors as summarized in Eq. (26).

In the symmetric case ($c=0$), a fractional power series expansion of the two normalized eigenvectors looks different. The result is

$$\boldsymbol{x}_1(\varphi)=\begin{pmatrix}\frac{e^{i7\pi/8}}{2^{3/4}}\frac{e^{-i\varphi/4}}{\varrho^{1/4}}+\frac{e^{i9\pi/8}}{2^{5/4}}\varrho^{1/4}e^{i\varphi/4}+O(\varrho^{3/4})\\ \frac{e^{i11\pi/8}}{2^{3/4}}\frac{e^{-i\varphi/4}}{\varrho^{1/4}}+\frac{e^{i5\pi/8}}{2^{5/4}}\varrho^{1/4}e^{i\varphi/4}+O(\varrho^{3/4})\end{pmatrix},$$

$$\boldsymbol{x}_2(\varphi)=\begin{pmatrix}\frac{e^{i11\pi/8}}{2^{3/4}}\frac{e^{-i\varphi/4}}{\varrho^{1/4}}+\frac{e^{i5\pi/8}}{2^{5/4}}\varrho^{1/4}e^{i\varphi/4}+O(\varrho^{3/4})\\ \frac{e^{i15\pi/8}}{2^{3/4}}\frac{e^{-i\varphi/4}}{\varrho^{1/4}}+\frac{e^{i\pi/8}}{2^{5/4}}\varrho^{1/4}e^{i\varphi/4}+O(\varrho^{3/4})\end{pmatrix}.$$

With a circle around the exceptional point ($\varphi=0\cdots 2\pi$) it can be seen directly that $\boldsymbol{x}_1(2\pi)=-\boldsymbol{x}_2(0)$ and $\boldsymbol{x}_2(2\pi)=\boldsymbol{x}_1(0)$, i.e., the permutation rule (26) for a symmetric matrix is reproduced in this picture.

[1] F. Dalfovo and S. Stringari, Phys. Rev. A **53**, 2477 (1996).
[2] R. J. Dodd, M. Edwards, C. J. Williams, C. W. Clark, M. J. Holland, P. A. Ruprecht, and K. Burnett, Phys. Rev. A **54**, 661 (1996).
[3] V. M. Pérez-García, H. Michinel, J. I. Cirac, M. Lewenstein, and P. Zoller, Phys. Rev. A **56**, 1424 (1997).
[4] C. C. Bradley, C. A. Sackett, and R. G. Hulet, Phys. Rev. Lett. **78**, 985 (1997).
[5] C. A. Sackett, J. M. Gerton, M. Welling, and R. G. Hulet, Phys. Rev. Lett. **82**, 876 (1999).
[6] J. M. Gerton, D. Strekalov, I. Prodan, and R. G. Hulet, Nature (London) **408**, 692 (2000).
[7] E. A. Donley, N. R. Claussen, S. L. Cornish, J. L. Roberts, E. A. Cornell, and C. E. Wieman, Nature (London) **412**, 295 (2001).
[8] C. Huepe, S. Métens, G. Dewel, P. Borckmans, and M. E. Brachet, Phys. Rev. Lett. **82**, 1616 (1999).
[9] C. Huepe, L. S. Tuckerman, S. Métens, and M. E. Brachet, Phys. Rev. A **68**, 023609 (2003).
[10] I. Papadopoulos, P. Wagner, G. Wunner, and J. Main, Phys. Rev. A **76**, 053604 (2007).
[11] D. O'Dell, S. Giovanazzi, G. Kurizki, and V. M. Akulin, Phys. Rev. Lett. **84**, 5687 (2000).
[12] T. Kato, *Perturbation Theory for Linear Operators* (Springer, Berlin, 1966).
[13] M. V. Berry and D. H. J. O'Dell, J. Phys. A **31**, 2093 (1998).
[14] W. D. Heiss and A. L. Sannino, Phys. Rev. A **43**, 4159 (1991).
[15] W. D. Heiss, Eur. Phys. J. D **7**, 1 (1999).
[16] A. L. Shuvalov and N. H. Scott, Acta Mech. **140**, 1 (2000).
[17] W. D. Heiss and H. L. Harney, Eur. Phys. J. D **17**, 149 (2001).
[18] M. V. Berry and M. R. Dennis, Proc. R. Soc. London, Ser. A **459**, 1261 (2003).
[19] U. Günther, I. Rotter, and B. F. Samsonov, J. Phys. A **40**, 8815 (2007).
[20] F. Keck, H. J. Korsch, and S. Mossmann, J. Phys. A **36**, 2125 (2003).
[21] M. Philipp, P. von Brentano, G. Pascovici, and A. Richter, Phys. Rev. E **62**, 1922 (2000).
[22] C. Dembowski, H.-D. Gräf, H. L. Harney, A. Heine, W. D. Heiss, H. Rehfeld, and A. Richter, Phys. Rev. Lett. **86**, 787 (2001).
[23] C. Dembowski, B. Dietz, H.-D. Gräf, H. L. Harney, A. Heine, W. D. Heiss, and A. Richter, Phys. Rev. Lett. **90**, 034101 (2003).
[24] T. Stehmann, W. D. Heiss, and F. G. Scholtz, J. Phys. A **37**, 7813 (2004).
[25] M. K. Oberthaler, R. Abfalterer, S. Bernet, J. Schmiedmayer, and A. Zeilinger, Phys. Rev. Lett. **77**, 4980 (1996).
[26] O. Latinne, N. J. Kylstra, M. Dörr, J. Purvis, M. Terao-Dunseath, C. J. Joachain, P. G. Burke, and C. J. Noble, Phys. Rev. Lett. **74**, 46 (1995).
[27] H. J. Korsch and S. Mossmann, J. Phys. A **36**, 2139 (2003).

[28] E. Hernández, A. Jáuregui, and A. Mondragón, J. Phys. A **39**, 10087 (2006).
[29] H. Cartarius, J. Main, and G. Wunner, Phys. Rev. Lett. **99**, 173003 (2007).
[30] A. P. Seyranian, O. N. Kirillov, and A. A. Mailybaev, J. Phys. A **38**, 1723 (2005).
[31] A. A. Mailybaev, O. N. Kirillov, and A. P. Seyranian, Phys. Rev. A **72**, 014104 (2005).
[32] W. D. Heiss, J. Phys. A **37**, 2455 (2004).
[33] H. L. Harney and W. D. Heiss, Eur. Phys. J. D **29**, 429 (2004).
[34] W. D. Heiss, J. Phys. A **39**, 10077 (2006).
[35] M. V. Berry, J. Phys. A **39**, 10013 (2006).
[36] N. Moiseyev and L. S. Cederbaum, Phys. Rev. A **72**, 033605 (2005).
[37] P. Schlagheck and T. Paul, Phys. Rev. A **73**, 023619 (2006).
[38] N. Moiseyev, Phys. Rep. **302**, 212 (1998).
[39] W. P. Reinhardt, Annu. Rev. Phys. Chem. **33**, 223 (1982).
[40] G. E. Cragg and A. K. Kerman, Phys. Rev. Lett. **94**, 190402 (2005).
[41] N. R. Claussen, E. A. Donley, S. T. Thompson, and C. E. Wieman, Phys. Rev. Lett. **89**, 010401 (2002).